

# Submesoscale streamers exchange water on the north wall of the Gulf Stream

Jody M. Klymak<sup>1</sup>, R. Kipp Shearman<sup>2</sup>, Jonathan Gula<sup>3</sup>, Craig M. Lee<sup>4</sup>, Eric A. D'Asaro<sup>4</sup>, Leif N. Thomas<sup>5</sup>, Ramsey R. Harcourt<sup>4</sup>, Andrey Y. Shcherbina<sup>4</sup>, Miles A. Sundermeyer<sup>6</sup>, Jeroen Molemaker<sup>7</sup>, and James C. McWilliams<sup>7</sup>

<sup>1</sup>University of Victoria, Victoria, British Columbia, Canada

<sup>2</sup>Oregon State University, Corvallis, Oregon, USA

<sup>3</sup>Laboratoire de Physique des Océans, Université de Bretagne Occidentale

<sup>4</sup>Applied Physics Laboratory, University of Washington, Seattle,  
Washington USA

<sup>5</sup>Stanford University, Stanford, California, USA

<sup>6</sup>University of Massachusetts Dartmouth, Dartmouth, Massachusetts, USA

<sup>7</sup>University of California, Los Angeles, California, USA

17 January 5, 2016

## Abstract

The Gulf Stream is a major conduit of warm surface water from the tropics to the subpolar North Atlantic. Large mesoscale ( $> 20$  km) “rings” often pinch off, but like the Gulf Stream they are resistant to lateral mixing, and retain their properties for a long time. Here we observe and simulate a sub-mesoscale ( $< 20$  km) mechanism by which the Gulf Stream exchanges water with the cold subpolar water to the north. The front exhibits a strong temperature-salinity contrast, with a distinct mode of “mixed” water between the two water masses that is between 2 and 4 km wide. This mass of water is not seen to increase downstream despite there being substantial energy available for mixing. A series of “streamers” detrain some of this water from the Gulf Stream at the crest of meanders. Subpolar water is entrained replacing the mixed water, and helping to resharpen the front. The water mass exchange can account for a northwards flux of salt of  $0.8 - 5$  psu m $^2$ s $^{-1}$ , which can be cast as an effective local diffusivity of  $O(100$  m $^2$ s $^{-1}$ ). This is similar to bulk-scale flux estimates of 1.2 psu m $^2$ s $^{-1}$  and supplies fresh water to the Gulf Stream required for the production of 18-degree subtropical mode water.

36        The Gulf Stream (GS) is the western boundary current of the North Atlantic  
37        subtropical wind-driven circulation. It separates from Cape Hatteras where  
38        it flows eastward into the North Atlantic. As it flows, it loses heat to the  
39        atmosphere and by mixing with the cold water in the subpolar gyre to the  
40        north. It also becomes fresher, an observation that can only be explained by  
41        entrainment of fresh water from the north [1]. As it entrains water, the GS  
42        increases its eastward transport by approximately  $4 - 8 \times 10^6 \text{ m}^3 \text{s}^{-1}/100 \text{ km}$   
43        (Johns et. al.[2]).

44        The GS has a sharp density front, but it also has a sharp temperature and  
45        salinity front, as has been demonstrated at the surface from shipboard surveys[3]  
46        and satellite images[4]. The sharpness of the front beneath the surface has  
47        been less-clear, and requires high-resolution lateral sampling to resolve. It is  
48        also known that the front has a sharp potential vorticity gradient[5], and such  
49        gradients act as a barrier to lateral mixing[6, 7]. Despite this barrier, property  
50        budgets indicate that there is significant exchange across the north wall[1], and  
51        that entrainment of fresh water is necessary to create the dynamically important  
52        “18-degree water” that fills much of the upper Sargasso Sea.

53        The mechanisms controlling this lateral mixing have not been identified.  
54        There are large eddies that periodically pinch off the GS and carry warm water  
55        to the north. However, some of these are re-entrained into the GS and do not  
56        result in a net exchange. Instead, tracer budgets across the front appear to be  
57        dominated by small-scale processes[8]. To date some of the best direct evidence  
58        for cross-front exchange consists of the trajectories of density-following floats  
59        placed at the north wall [9, 10]. These floats were observed to regularly detrain  
60        from the GS, such that of 95 floats, 26 stayed in the GS, 7 were detrain in rings,  
61        and 62 were detrained by mechanisms other than rings[10]. Kinematic theories  
62        have been examined to explain the detrainment of the floats [11, 12, 13], and  
63        the similarity to satellite images of “streamers” of warm water detraining from  
64        the Gulf Stream has been noted. However, direct observations of the processes  
65        as it occurs at depth have been lacking.

66        Here we present indirect evidence that there is small-scale mixing ( $<0.5 \text{ km}$ )  
67        on the northern cyclonic side of the GS, and that the mixed water periodically  
68        peels off the GS in thin (5-10 km wide) “streamers”. In March 2012 we made  
69        high-resolution measurements of the north wall of the GS from 66 W to 60 W  
70        (Fig. 1), about 850 km east of where the GS separates from the North American  
71        continental slope. Two research vessels tracked a water-following float placed in  
72        the GS front and programmed to follow the density of the surface mixed layer.  
73        The float was transported downstream with a speed of  $1.4 \pm 0.2 \text{ m s}^{-1}$ , in water  
74        that became denser as the surface of the GS cooled. One vessel maintained tight  
75        sampling around the float and deployed an undulating profiler to 200 m, making  
76        10-km cross sections every 10 km downstream. The second vessel had an  
77        undulating profiler making larger 30-km scale sections. Both profilers measured  
78        temperature, salinity and pressure, and had approximately 1-km along-track  
79        resolution; both ships also measured ocean currents. Fluorescent dye was de-  
80        ployed near the floats on some deployments, and measured by the profilers on  
81        the ships. By following the float, a focus on the front was maintained as it

82 curved and meandered to the east.

83 During these observations, the GS had a shallow meander crest at 65 W  
84 (Fig. 1b) followed by a long concave region (63 W) and then another large crest  
85 (61 W). Satellite measurements show the sharp temperature changes across the  
86 front, superimposed with thin intermediate-temperature (15-18°C) streamers  
87 detraining to the north at approximately 65 W, 64 W, and at the crest of the  
88 large meander at 61 W. An older streamer that has rolled up can also be seen at  
89 62 W. The ships passed through the three newer streamers providing the first  
90 detailed observations of their underwater structure.

91 The front consists of density surfaces that slope up towards the north (Fig. 2a-  
92 d). The water along density surfaces is saltier (and warmer) in the GS, and  
93 fresher (and colder) to the north. The transition between the two water masses  
94 is remarkably abrupt, occurring over less than 5-km. This sharpness per-  
95 sisted from our western-most section during the cruise (71.5 W) to the eastern-  
96 most (60.5 W). Some cross sections clearly show lateral interleaving of salinity  
97 north of the front (Fig. 2a) with approximately 5-km wide salinity anomalies  
98 ( $S \approx 36.15$  psu). These anomalies move slower than the front (Fig. 2e), and  
99 have high potential vorticity that is normally associated with the front (Fig. 2i).

100 The temperature-salinity (T/S) relationship of this data shows the contrast  
101 between the GS and the subpolar water as two distinct modes (Fig. 3a), except  
102 near the surface where the water masses are strongly affected by the atmosphere.  
103 For the deeper water, there is a third distinct population between the two larger  
104 modes in T/S space that represents the water in the salinity anomalies, and we  
105 have labelled as “streamers”. The distinctness in T/S space of the streamers  
106 indicates that after the GS and subpolar waters mixed, the partially mixed water  
107 continued to mix, condensing it in T/S space (perfectly mixed water would be  
108 a dot).

109 Looking at the GS in plan view (Fig. 3b) we see the mixed water that that  
110 makes up the streamers is connected along the length of our observations. The  
111 first streamer (64.5 W) is horizontally connected over 100 km, and is about 5  
112 km wide, and at least 150 m deep. Where the streamer is the most detached  
113 (Fig. 2a) the main front is the sharpest of the 4 cross sections. Downstream  
114 of this streamer, the mixed water thins before the eastern meander (60.5 W)  
115 where there is a second streamer. Further downstream, the mixed water almost  
116 disappears by the last cross-section (59 W).

117 We can quantify the rate of detrainment from the first streamer (64.5 W). It  
118 starts on the fast side of the front with water flowing approximately  $0.25 \text{ m s}^{-1}$   
119 faster than the float (Fig. 2h). Upstream, where it is detached (Fig. 2e), it is  
120 flowing almost  $0.5 \text{ m s}^{-1}$  slower than the float. A 5-km wide and 150-m deep  
121 streamer, with a relative velocity of  $0.75 \text{ m s}^{-1}$  represents a rate of detrainment  
122 of over  $0.5 \times 10^6 \text{ m}^3 \text{ s}^{-1}$ .

123 Concurrently, there is a bolus of fresh water from the north that is enfolded  
124 between the streamers and the GS, which we will call an “intrusion”. The  
125 entrainment of the intrusion is hard to quantify using the data presented above,  
126 because it is drawn from a large pool of water upstream. However, a subsequent  
127 survey of the north wall (March 14) included a dye release in this water that was

128 observed to be entrained in an intrusion (Fig. 4a-c). The streamer during this  
129 occupation was less pronounced than the one described above, but was clear for  
130 a number of passes through the north wall. The dye cloud was quite spread out,  
131 but the data show clear interleaving of the intrusion water.

132 High-resolution numerical simulations ( $dx \approx 500m$ , see Methods) resolve  
133 these features and also confirm the entrainment of the fresh intrusion (Fig. 4d-  
134 i). Seeding the simulation with Lagrangian particles (see methods) allows us to  
135 track the evolution of the streamers and the intrusion as the flow moves down-  
136 stream. Before the streamer is formed, the water in the intrusion (magenta  
137 contours) is near the surface and the streamer water (green contours) is well  
138 within the front (Fig. 4d,g). Downstream (Fig. 4e,h) the fresh water has been  
139 subducted to 150 m depth, and the streamer has been pushed north of the front.  
140 Both water masses accelerate with the GS (Fig. 4f), but the fresh intrusion ac-  
141 celerates more, such that the intrusion is entrained and the streamer slows and is  
142 detrain. As in the observations, the streamer occupies an intermediate region  
143 in T-S space (Fig. 4i, green contour), and originates in the high-vorticity region  
144 of the front. The acceleration of the fresh intrusion relative to the streamer is  
145 an important finding of the model, as the fresh water now forms a new sharp  
146 T-S front with the warm salty GS, and the mixed streamer water is carried away  
147 from the front. The model further shows that the streamers are more prominent  
148 on the leading edges of meanders, also clearly seen in satellite images (Fig. 1).

149 There are two major implications of the loss of mixed water to the north.  
150 The first is that it helps explain why the front at the north wall of the GS  
151 remains so sharp. The T/S distribution clearly indicate that there is mixing  
152 because of the separate water-class mode. However we also show that the mixing  
153 product is carried away in the streamers. It is striking that it is only the mixed  
154 water that is carried away, and not high-salinity GS water (Fig. 3b). This  
155 implies a dynamical link that we have not seen explored. Streamers have been  
156 observed in surface temperature satellite images and indirectly by subsurface  
157 floats[9, 11, 14, 15], and this has led to kinematic models in which particles are  
158 displaced from streamlines going around propagating meanders [16, 13, 14]. The  
159 observations here add to these models by showing that it is only mixed water  
160 that leaves the GS. This co-incidence indicates to us a role for small-scale mixing  
161 in producing the destabilizing forces that cause this water to detrain from the  
162 north wall. The observations and simulation indicate that the meanders of the  
163 GS play an important role in the formation of the streamers.

164 The second implication is that the streamers are a mechanism that can  
165 balance large-scale budgets that require significant exchange across the GS[1, 8].  
166 Such budgets suggest that this region of the GS loses salinity to the north at a  
167 rate of  $1.2 \text{ psu } \text{m}^2 \text{s}^{-1}$  [1]. Each streamer transports  $0.2 - 0.5 \times 10^6 \text{ m}^3 \text{s}^{-1}$  of water  
168 that is  $0.8 - 1 \text{ psu}$  saltier than the water that is entrained. Streamers appear  
169 approximately every 100-300 km, associated with meanders, so an estimate of  
170 their average transport is  $0.8 - 5 \text{ psu } \text{m}^2 \text{s}^{-1}$ , bracketing the large-scale estimates.  
171 Working against a gradient of  $1 \text{ psu}/10 \text{ km}$  over 200 m depth, the equivalent  
172 lateral diffusivity is  $40 - 250 \text{ m}^2 \text{s}^{-1}$ .

173 Here we have observed a submesoscale lateral stirring process along the

174 north wall of the GS. The T/S front remains persistently sharp, despite small-  
 175 scale mixing evident from the T/S diagrams, and due to a number of possible  
 176 processes[17, 18]. The mixed water mass does not accumulate, or it would  
 177 weaken the sharpness of the front. Here we show that the streamers detrain  
 178 mixed water, and entrain cold and fresh water toward the north wall, resharpening  
 179 the temperature-salinity front. Further analysis of the data and models  
 180 will shed light on the exact mechanism triggering the ejection of water from the  
 181 front via the streamers.

## 182 Methods

183 The Lagrangian float[19] was placed in the Gulf Stream front based on a brief  
 184 cross-stream survey, and programmed to match the density of the surface mixed  
 185 layer (upper 30 m). The float moved downstream at a mean speed of  $1.4 \text{ m s}^{-1}$ .  
 186 The *R/V Knorr* tracked the float and deployed a Chelsea Instruments TriAxus  
 187 that collected temperature, salinity, and pressure (CTD) on a 200-m deep saw-  
 188 tooth with approximately 1-km lateral spacing in a 10-km box-shaped pattern  
 189 relative to the float (Fig. 1, magenta). *R/V Atlantis* performed larger cross  
 190 sections approximately 30 km across the front, trying to intercept the float on  
 191 each front crossing. *R/V Atlantis* was deploying a Rolls Royce Marine Mov-  
 192 ing Vessel Profiler equipped with a CTD that profiled to 200 m approximately  
 193 every 1 km. Both ships had a 300 kHz RDI Acoustic Doppler Current Pro-  
 194 filer (ADCP) collecting currents on 2-m vertical scale averaged every 5 minutes  
 195 (approximately 1 km lateral scale), collected and processed using UHDAS and  
 196 CODAS (<http://currents.soest.hawaii.edu>[20]). This data reached about 130 m,  
 197 and was supplemented at deeper depths with data from 75 kHz RDI ADCPs,  
 198 with 8-m vertical resolution.

199 Data were interpolated onto depth surfaces by creating a two-dimensional  
 200 interpolation onto a grid via Delauney triangulation. No extrapolation was  
 201 performed. Data on the  $26.25 \text{ kg m}^{-3}$  isopycnal were assembled at each grid  
 202 point by finding the first occurrence of that isopycnal in depth.

203 Potential vorticity is calculated from the three-dimensional grid as

$$q = -\frac{g}{\rho_0} (\nabla \times \mathbf{u} + \mathbf{f}) \cdot \nabla \rho, \quad (1)$$

204 where  $f$  is the Coriolis frequency,  $g$  the gravitational acceleration. The brack-  
 205 eted term is twice the angular velocity, including the planet's rotation, and the  
 206 gradient of density represents the stretching or compression of the water col-  
 207 umn. In the GS, the potential vorticity is dominated by contributions from  
 208 the vertical density gradient and the cross-stream gradient of the along-stream  
 209 velocity:

$$q \approx N^2 \left( -\frac{\partial u}{\partial y} + f \right). \quad (2)$$

210 Dye Release. At select times during the float evolutions, fluorescein dye  
 211 releases (100 kg per release) were conducted at depth as close as possible to the

212 float. Dye was pumped down a hose to a tow package deployed off the side of  
213 the ship, consisting of a CTD and a dye diffuser. Prior to injection, the dye was  
214 mixed with alcohol and ambient sea water to bring it to within  $0.001 \text{ kg m}^{-3}$   
215 of the float's target density. Initial dimensions of the dye streak were  $\approx 1 \text{ km}$   
216 along-stream,  $\approx 100 \text{ m}$  cross-stream (after wake adjustment), and ranging from  
217 1 - 5 m in the vertical. The TriAxus system on the *R/V Knorr* tracked the  
218 fluorescein from its CTD package.

219 Numerical simulation. The high-resolution realistic simulation of the GS  
220 is performed with the Regional Oceanic Modeling System (ROMS[21]). This  
221 simulation has a horizontal resolution of 500m and 50 vertical levels. The model  
222 domain spans 1,000 km by 800 km and covers a region of the GS downstream  
223 from its separation from the U.S. continental slope. Boundary conditions are  
224 supplied by a sequence of two lower-resolution simulations that span the entire  
225 GS region and the Atlantic basin, respectively. The simulation is forced by  
226 daily winds and diurnally modulated surface fluxes. The modelling approach is  
227 described in detail in Gula et. al[22].

228 Virtual Lagrangian Particles. Neutrally buoyant Lagrangian (flow-following)  
229 particles were seeded at time 285 and advected both backwards and forwards  
230 from this time by the model velocity fields without additional dispersion from  
231 the model's mixing processes[23]. A 4th-order Runge-Kutta method with a time  
232 step  $dt = 1 \text{ s}$  is used to compute particle advection. Velocity and tracer fields  
233 are interpolated at the positions of the particles using cubic spline interpolation  
234 in both the horizontal and vertical directions. We use hourly outputs from the  
235 simulation to get sufficiently frequent and temporally-smooth velocity sampling  
236 for accurate parcel advection.

## 237 References

- 238 [1] Joyce, T. M., Thomas, L. N., Dewar, W. K. & Girton, J. B. Eighteen  
239 degree water formation within the Gulf Stream during CLIMODE. *Deep*  
240 *Sea Res. II* (2013).
- 241 [2] Johns, W., Shay, T., Bane, J. & Watts, D. Gulf Stream structure, trans-  
242 port, and recirculation near 68 W. *J. Geophys. Res.* **100**, 817–817 (1995).
- 243 [3] Ford, W., Longard, J. & Banks, R. On the nature, occurrence and origin  
244 of cold low salinity water along the edge of the Gulf Stream. *J. Mar. Res.*  
245 **11**, 281–293 (1952).
- 246 [4] Churchill, J. H., Cornillon, P. C. & Hamilton, P. Velocity  
247 and hydrographic structure of subsurface shelf water at the Gulf  
248 Stream's edge. *J. Geophys. Res.* **94**, 10791–10800 (1989). URL  
249 <http://dx.doi.org/10.1029/JC094iC08p10791>.
- 250 [5] Rajamony, J., Hebert, D. & Rossby, T. The cross-stream potential vorticity  
251 front and its role in meander-induced exchange in the Gulf Stream. *J. Phys.*  
252 *Oceanogr.* **31**, 3551–3568 (2001).

- 253 [6] Marshall, J., Shuckburgh, E., Jones, H. & Hill, C. Estimates and implications  
 254 of surface eddy diffusivity in the Southern Ocean derived from tracer  
 255 transport. *J. Phys. Oceanogr.* **36**, 1806–1821 (2006).
- 256 [7] Naveira Garabato, A. C., Ferrari, R. & Polzin, K. L. Eddy stirring in the  
 257 Southern Ocean. *J. Geophys. Res.* **116** (2011).
- 258 [8] Bower, A. S., Rossby, H. T. & Lillibridge, J. L. The Gulf Stream-barrier  
 259 or blender? *J. Phys. Oceanogr.* **15**, 24–32 (1985).
- 260 [9] Bower, A. & Rossby, T. Evidence of cross-frontal exchange processes in  
 261 the Gulf Stream based on isopycnal RAFOS float data. *J. Phys. Oceanogr.*  
 262 **19**, 1177–1190 (1989).
- 263 [10] Bower, A. S. & Lozier, M. S. A closer look at particle exchange in the Gulf  
 264 Stream. *J. Phys. Oceanogr.* **24**, 1399–1418 (1994).
- 265 [11] Flierl, G., Malanotte-Rizzoli, P. & Zabusky, N. Nonlinear waves and co-  
 266 herent vortex structures in barotropic  $\beta$ -plane jets. *J. Phys. Oceanogr.* **17**,  
 267 1408–1438 (1987).
- 268 [12] Stern, M. E. Lateral wave breaking and “shingle” formation in large-scale  
 269 shear flow. *J. Phys. Oceanogr.* **15**, 1274–1283 (1985).
- 270 [13] Pratt, L. J., Susan Lozier, M. & Beliakova, N. Parcel trajectories in quasi-  
 271 geostrophic jets: Neutral modes. *J. Phys. Oceanogr.* **25**, 1451–1466 (1995).
- 272 [14] Lozier, M., Pratt, L., Rogerson, A. & Miller, P. Exchange geometry re-  
 273 vealed by float trajectories in the Gulf Stream. *J. Phys. Oceanogr.* **27**,  
 274 2327–2341 (1997).
- 275 [15] Song, T., Rossby, T. & Carter, E. Lagrangian studies of fluid exchange  
 276 between the Gulf Stream and surrounding waters. *J. Phys. Oceanogr.* **25**,  
 277 46–63 (1995).
- 278 [16] Bower, A. S. A simple kinematic mechanism for mixing fluid parcels across  
 279 a meandering jet. *J. Phys. Oceanogr.* **21**, 173–180 (1991).
- 280 [17] Thomas, L. N. & Shakespeare, C. A new mechanism for mode water for-  
 281 mation involving cabbeling and frontogenetic strain at thermohaline fronts.  
 282 In press *J. Phys. Oceanogr.*
- 283 [18] Whitt, D. B. & Thomas, L. N. Near-inertial waves in strongly baroclinic  
 284 currents. *J. Phys. Oceanogr.* **43**, 706–725 (2013).
- 285 [19] D’Asaro, E. A. Performance of autonomous Lagrangian floats. *J. Atmos.*  
 286 *Ocean. Tech.* **20**, 896–911 (2003).
- 287 [20] Firing, E., Hummon, J. M. & Chereskin, T. K. Improving the quality  
 288 and accessibility of current profile measurements in the Southern Ocean.  
 289 *Oceanography* (2012).

- <sup>290</sup> [21] Shchepetkin, A. & McWilliams, J. The regional oceanic modeling sys-  
<sup>291</sup> tem (ROMS): a split-explicit, free-surface, topography-following-coordinate  
<sup>292</sup> oceanic model. *Ocean Modell.* **9**, 347–404 (2005).
- <sup>293</sup> [22] Gula, J., Molemaker, M. J. & McWilliams, J. C. Gulf Stream dynam-  
<sup>294</sup> ics along the southeastern US seaboard. *J. Phys. Oceanogr.* **45**, 690–715  
<sup>295</sup> (2015).
- <sup>296</sup> [23] Gula, J., Molemaker, M. J. & McWilliams, J. C. Submesoscale cold fila-  
<sup>297</sup> ments in the Gulf Stream. *J. Phys. Oceanogr.* **44**, 2617–2643 (2014).

298 **List of Figures**

- 299 1 **Experimental design.** Inset: The experiment site on the north  
300 wall of the Gulf Stream, between 66 and 60 W, as shown in an  
301 AVHRR satellite image of sea surface temperature (SST). Main:  
302 Detailed SST image composed from two satellite images. The  
303 GS is warm and delineated by a sharp front. The small sub-  
304 mesoscale structures north of the front are the focus of this paper.  
305 The satellite images are a composite from early in the observation  
306 period (AVHRR 6 Mar), and late (MODIS, 9 Mar). A Lagrangian  
307 float was deployed in the front (black curve), and the ship tracks  
308 bracketed the float's position (green: *R/V Atlantis*, magenta:  
309 *R/V Knorr*). *R/V Atlantis* cross-sections labeled a-d are shown  
310 in Fig. 2a-d. . . . . 311 13
- 311 2 **Cross sections of data collected across the Gulf Stream.**  
312  $Y$  is the cross-stream distance perpendicular to the path of the  
313 float, positive being northwards. The four columns correspond  
314 to the four sections labeled a-d in Fig. 1. Potential density is  
315 contoured in black and  $\sigma_0 = 26.25 \text{ kg m}^{-3}$  is magenta. Along a  
316 constant density surface salty water is warmer than fresher water,  
317 so the GS on the left is warm and salty. Section a) is the fur-  
318thest upstream section (65W) and d) is the furthest downstream  
319 (63.75 W) (Fig. 3b). e)-h) downstream velocity calculated rela-  
320 tive to the float's trajectory by removing the float's mean speed  
321 of  $u_{\text{float}} = 1.4 \text{ m s}^{-1}$  for the observation period. Green contours  
322 are regions in temperature-salinity space labeled "streamers" in  
323 Fig. 3a. i)-l) Potential vorticity (see methods); . . . . . 324 14



4 **Evidence for entrainment of intrusions from a dye re-**  
344 **lease and numerical simulation.** a) Salinity section from  
345 an occupation of the GS 14 March. The location of a dye is  
346 contoured in magenta. b) Salinity section from downstream. A  
347 streamer has enfolded the dye in cold-fresh water between itself  
348 and the GS. c) Temperature-salinity diagram for this occupa-  
349 tion. The temperature-salinity for the dye is coloured in dark  
350 magenta. d) Salinity in the GS on the  $\sigma_\theta = 26.25 \text{ kg m}^{-3}$  isopyc-  
351 nals from a high-resolution numerical simulation at  $t_0$ . The green  
352 contours delineate the location of particles seeded downstream in  
353 the streamer at time  $t_1 = t_0 + 70\text{h}$  (see panels e and h) and ad-  
354 vected *backwards* in time to  $t_0$  showing where the streamer water  
355 originated. The dark magenta contour is the location of particles  
356 seeded in the fresh intrusion. The straight line shows the location  
357 of the salinity cross-section in panel g. e) as panel d, except at  
358  $t_1 = t_0 + 70\text{ h}$ ; this is the time and locations where the two clouds  
359 of particles were seeded. g) and h) salinity cross sections for times  
360  $t_0$  and  $t_1$ . The location of the particles is shown in green and dark  
361 magenta contours. The the  $\sigma_\theta = 26.25 \text{ kg m}^{-3}$  isopycnal is  
362 contoured in light magenta. These panels show that the origin of the  
363 streamer water was in the GS front, and that the fresh-cold water  
364 (magenta contour) enfolded against the front came from north of  
365 the front. f) shows the speeds of the particle clouds in time, and  
366 shows that the intrusion water (magenta) accelerates relative to  
367 the streamer water (green). i) The temperature-salinity of all  
368 the data at  $t_1$ , with the clouds of seeded particles indicated in  
369 T/S space. Note that the green streamer water occupies a mixed  
370 mode between the warm GS waters and the cold and fresh water  
371 to the north.

373 **Acknowledgements** Our thanks to the captains and crews of *R/V Knorr*  
374 and *R/V Atlantis*, The AVHRR Oceans Pathfinder SST data were obtained from  
375 the Physical Oceanography Distributed Active Archive Center (PO.DAAC) at  
376 the NASA Jet Propulsion Laboratory, Pasadena, CA. <http://podaac.jpl.nasa.gov>.  
377 The bulk of this work was funded under the Scalable Lateral Mixing and Co-  
378 herent Turbulence Departmental Research Initiative and the Physical Oceanog-  
379 raphy Program.

380 **Author Contributions** JMK did the main analysis of the data and wrote  
381 the paper. JMK, CL, EAD, KS, MS, AS, LT collected the data, performed  
382 quality control. RH supplied satellite imagery both at sea and on land. JG,  
383 JM and JM ran the simulations and analyzed them. All authors contributed  
384 significantly to the analysis and interpretation of these results.

385 **Competing Interests** The authors declare that they have no competing fi-  
386 nancial interests.

387 **Correspondence** Correspondence and requests for materials should be ad-  
388 dressed to Jody Klymak. (email: [jklymak@uvic.ca](mailto:jklymak@uvic.ca)).

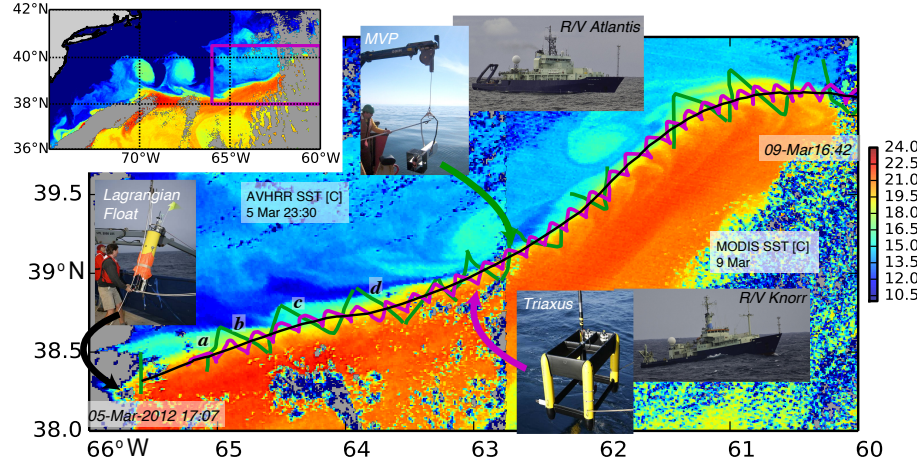


**Figure 1: Experimental design.** Inset: The experiment site on the north wall of the Gulf Stream, between 66 and 60 W, as shown in an AVHRR satellite image of sea surface temperature (SST). Main: Detailed SST image composed from two satellite images. The GS is warm and delineated by a sharp front. The small sub-mesoscale structures north of the front are the focus of this paper. The satellite images are a composite from early in the observation period (AVHRR 6 Mar), and late (MODIS, 9 Mar). A Lagrangian float was deployed in the front (black curve), and the ship tracks bracketed the float's position (green: *R/V Atlantis*, magenta: *R/V Knorr*). *R/V Atlantis* cross-sections labeled a-d are shown in Fig. 2a-d.

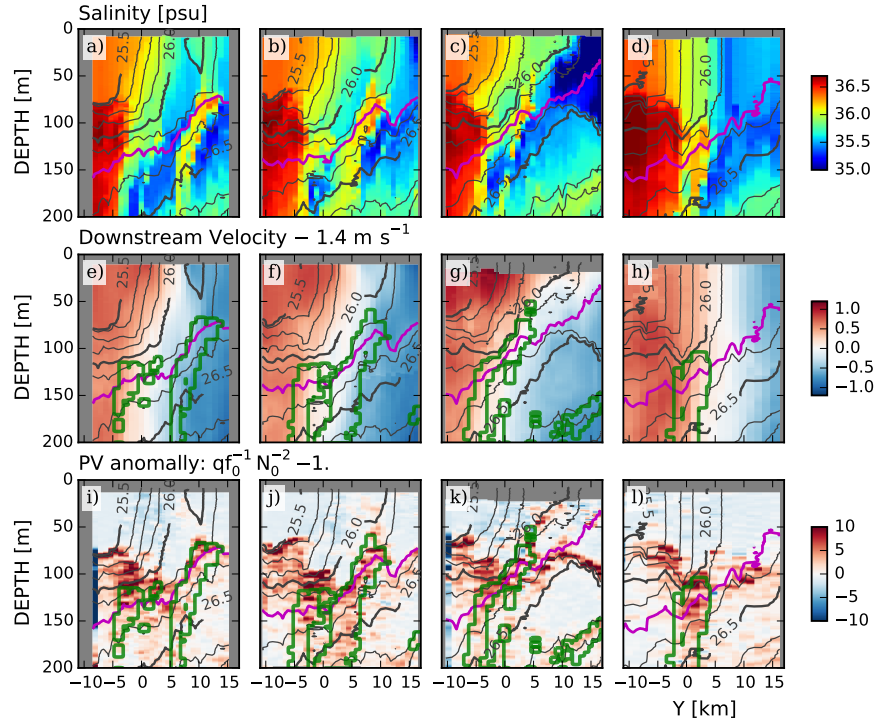


**Figure 2: Cross sections of data collected across the Gulf Stream.**  $Y$  is the cross-stream distance perpendicular to the path of the float, positive being northwards. The four columns correspond to the four sections labeled a-d in Fig. 1. Potential density is contoured in black and  $\sigma_\theta = 26.25 \text{ kg m}^{-3}$  is magenta. Along a constant density surface salty water is warmer than fresher water, so the GS on the left is warm and salty. Section a) is the furthest upstream section (65W) and d) is the furthest downstream (63.75 W) (Fig. 3b). e)–h) downstream velocity calculated relative to the float’s trajectory by removing the float’s mean speed of  $u_{\text{float}} = 1.4 \text{ m s}^{-1}$  for the observation period. Green contours are regions in temperature-salinity space labeled “streamers” in Fig. 3a. i)–l) Potential vorticity (see methods);

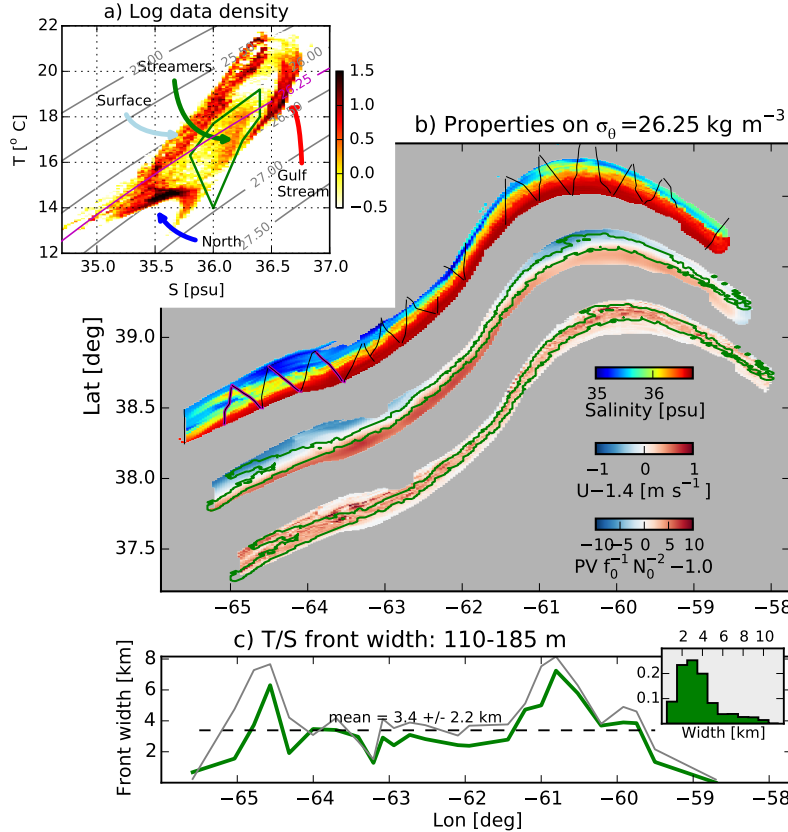


**Figure 3: Streamer properties and distribution in space.** a) Logarithmically scaled histogram in temperature-salinity space (colours). The warm-salty GS water is distinct from the water to the north, which is cold and fresh. The water near the surface is heavily modified by the atmosphere. Deeper, there is a class of water distinct from the GS water and the water to the north, that we label “streamers”. This water is contoured in green in Fig. 2e-l. b) Interpolation of salinity, velocity, and potential vorticity onto the  $\sigma_\theta = 26.25 \text{ kg m}^{-3}$  isopycnal, plotted geographically (with a small exaggeration of scale in the north-south direction, and the latter two fields offset slightly to the south-east). This used data from both ships. The ship track for the *Atlantis* is plotted in black, and the four cross-sections in Fig. 2 are plotted in magenta. The streamer water is contoured in green. c) The width of the T/S front attached to the north wall, averaged between 110 and 185 m (green line). The grey line is the width of all the water in the “streamer” T/S class. A water parcel is considered “attached” if there is no more than one kilometer of water from the fresher water class to the north. This is meant to exclude the clearly detached streamers.

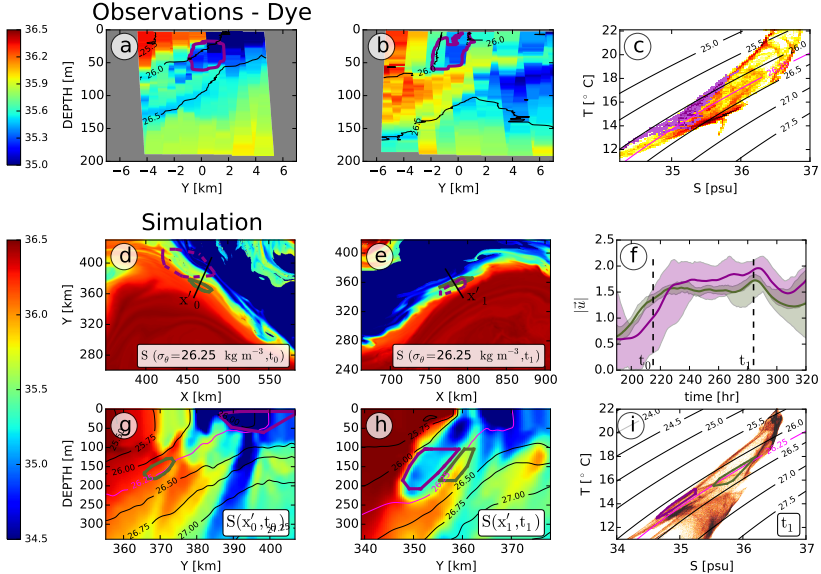


**Figure 4: Evidence for entrainment of intrusions from a dye release and numerical simulation.** a) Salinity section from an occupation of the GS 14 March. The location of a dye is contoured in magenta. b) Salinity section from downstream. A streamer has enfolded the dye in cold-fresh water between itself and the GS. c) Temperature-salinity diagram for this occupation. The temperature-salinity for the dye is coloured in dark magenta. d) Salinity in the GS on the  $\sigma_\theta = 26.25 \text{ kg m}^{-3}$  isopycnal from a high-resolution numerical simulation at  $t_0$ . The green contours delineate the location of particles seeded downstream in the streamer at time  $t_1 = t_0 + 70\text{h}$  (see panels e and h) and advected *backwards* in time to  $t_0$  showing where the streamer water originated. The dark magenta contour is the location of particles seeded in the fresh intrusion. The straight line shows the location of the salinity cross-section in panel g. e) as panel d, except at  $t_1 = t_0 + 70\text{ h}$ ; this is the time and locations where the two clouds of particles were seeded. g) and h) salinity cross sections for times  $t_0$  and  $t_1$ . The location of the particles is shown in green and dark magenta contours. The the  $\sigma_\theta = 26.25 \text{ kg m}^{-3}$  isopycnal is contoured in light magenta. These panels show that the origin of the streamer water was in the GS front, and that the fresh-cold water (magenta contour) enfolded against the front came from north of the front. f) shows the speeds of the particle clouds in time, and shows that the intrusion water (magenta) accelerates relative to the streamer water (green). i) The temperature-salinity of all the data at  $t_1$ , with the clouds of seeded particles indicated in T/S space. Note that the green streamer water occupies a mixed mode between the warm GS waters and the cold and fresh water to the north.